PERGAMON International Journal of Engineering Science 40 (2002) 1113–1130

International Journal of Engineering Science

www.elsevier.com/locate/ijengsci

Thermoelastic contact of a rotating shaft with a rigid bush in conditions of bush wear and stick-slip movements

J. Awrejcewicz *, Yu. Pyryev

Department of Automatics and Biomechanics (K-16), Technical University of Łódź, 1/15 Stefanowskiego St., 90-924 Łódź, Poland

Received 11 May 2001; received in revised form 6 August 2001; accepted 17 September 2001

Abstract

The nonlinear problem of thermoelastic contact of a rotating shaft with a rigid bush fixed to the base elastically (springs) is investigated using both Laplace transform and perturbation methods. A friction coefficient is assumed to be a nonlinear function of a relative velocity. The solution to the problem is reduced to the system of nonlinear differential and integral equations. Zones of steady-state solution stability and friction self-excited oscillations existence are established. The numerical analysis is carried out and some important conclusions are given.

Keywords: Nonlinear thermoelastic contact; Self-excited oscillations; Stick-slip oscillations; Rotating shaft; Rigid bush

1. Introduction

Friction, wear, heat generation and temperature deformation are complex processes which influence each other and making up a sole diverse process of a friction unit work. During transient friction process time changes of all parameters of the problem are mutually connected and conditioned. During small sliding velocities rapid un-uniform movements can be observed very often. These movements take place intermittently with periodical disruptions and stops. In the considered paper we have made an attempt to investigate this mutual connection on the simplest model that remains in conditions of such relative movements as stick-slip oscillations.

Uneven movement during friction (stick-slip motion) is the phenomenon of alternate relative sliding and relative rest that arises due to self-oscillations during decreasing of friction coefficient while sliding velocity increases. The main reason of mechanical oscillations arising is presence of positive difference between friction force of rest and sliding. This difference is caused by the

* Corresponding author. Tel.: +48-4842-6312378; fax: +48-4842-6312225.

E-mail addresses: awrejcew@ck-sg.p.lodz.pl (J. Awrejcewicz), jupyrjew@ck-sg.p.lodz.pl (Y. Pyryev).

0020-7225/02/$ - see front matter
PII: S0020-7225(02)00008-3

decreasing of sliding friction force with the increasing of relative velocity. Self-oscillations are undamped oscillations supported by external energy sources in the nonlinear dissipative system. They principally differ from other oscillatory processes in dissipative systems in that way that the supporting periodical influence from outside is not necessary. Under wear process we will understand the process of material separation from the surface of the body that leads to gradual change of dimensions. Wear is the result of wear process that can be measured in the length units.

To the present time the different models of nonlinear mechanical systems frictional self-oscillations and the methods of their solving were considered in [1–6]. Investigation of dry friction is presented and the approaches for the evaluation of this kind of friction are developed in [3,4,7]. Friction units wear investigation is performed and corresponding methods of wear calculation are discussed in [7].

However, less investigated remains question concerning frictional oscillations in conditions of heat generation and wear. Investigation of such oscillations arising conditions and behavior of contact characteristics (contact temperature, contact pressure, wear) could be useful for the explanation of different phenomena in disk brakes, grinding machines, high accuracy mechanisms (when it is necessary to assure displacements with small velocities) and other machines with friction couples.

The problem related to oscillations of a spring fixed on the steady base bush with respect to uniformly rotating shaft in conditions of high friction is investigated in [6]. This problem can be treated as the draft sketch of ordinary braking pad or Prony's clamp. For small rotating velocity of a shaft a stick-slip motion of a braking pad is observed. For large velocities the pad undergoes the damped periodical oscillations. A similar behavior is also observed in many various models which are described and illustrated in [2–5]. As it is well known a decreasing part of the kinetic friction F_t^k versus (small) velocity is responsible for an occurrence of stick-slip oscillations [8–11].

Thermoelastic contact of a rotating shaft with an uninertial steady bush with wear processes is considered in works [12,13]. Observe that during shaft rotation its volume is extended due to occurrence of a heat process. On the other hand the process of material wear from the bush surface occurs. All of the contact characteristics of two sliding bodies are coupled. In addition, when so-called critical rotation velocity is achieved a surrounding medium does not keep up with heat collection and the system is overheated (the contact characteristics increase exponentially), and thermoelastic instability occurs. The mentioned bush wear process leads to increase of the critical velocity, and finally, for enough high wearing, the critical velocity does not appear. Dynamical models of thermoelastic contact in conditions of frictional heating are also presented in [14–19].

In the present work more general plane axially symmetric problem about thermoelastic contact of the rotating shaft with the rigid bush fixed elastically to the steady base by springs in conditions of frictional self-oscillations and wear is investigated. Observe that in our considered system a shaft temperature, the contact pressure, wear of the bush, and the bush movement of our system are coupled with each other. The paper is mainly focused on analysis of the mentioned self-coupling processes.

2. Statement of the problem

Consider thermoelastic contact of solid isotropic circular shaft (cylinder) of radius R_1 with a cylindrical tube-like rigid bush (solid liner, rigid ring) which is fitted to the cylinder according to the expression $U_0h(t)$ (Fig. 1). Calculated per unit of the length inertia moment of the bush is equal to B_2. Bush is fixed to the steady-state base through the spring with reduced coefficient of rigidity k_2. Shaft rotates with angular velocity $\Omega(t) = \Omega_*\omega_1(t)$. On the contact surface between the cylinder and the bush friction force F_t arises and as the consequence heat generation and wear U_z take place. The work of friction force is transformed into heat energy. The temperature of the shaft at the initial instant of time is equal to T_0. Assume that between shaft and the bush Newton's heat exchange law takes place and that the bush has constant temperature T_0.

Both thermal and stress–strain state of the shaft is considered using the cylinder co-ordinates R, ϕ, Z rotating with the angular velocity Ω with its origin situated in the center of the rotating elastic body. The governing equations of motion of uncoupled thermoelastic problem along Z axis have the following form [20,21]:

$$\mu\nabla^2\mathbf{u} + (\lambda+\mu)\,\mathrm{grad}\,\mathrm{div}\,\mathbf{u} + \rho\Omega^2 R\mathbf{e}_R = (3\lambda+2\mu)\alpha_1\,\mathrm{grad}\,T + \rho\frac{\partial^2\mathbf{u}}{\partial t^2}, \quad \nabla^2 T = \frac{1}{a_1}\frac{\partial T}{\partial t}, \tag{1}$$

where ∇^2 is the Laplace operator, $\mathbf{u} = U\mathbf{e}_R + V\mathbf{e}_\phi + W\mathbf{e}_Z$ the vector of relative displacement, T the bush temperature, λ, μ the Lamé coefficients, ρ the bush density, α_1 the coefficient of linear thermal expansion, and a_1 is the thermal diffusivity.

We consider the bush as an ideal rigid body and its movement is described using the cylinder co-ordinates R, φ_2, Z. A set of three Euler's equations are reduced to only one which can be presented as the following differential inclusion [4,22]:

$$B_2\ddot{\varphi}_2 + F_s R_2 \in F_t R_1, \tag{2}$$

where $\varphi_2(t)$ is the angle of bush deviation, $F_s = k_2\varphi_2 R_2$ springs force related to the bush unit length, F_t friction force acting on the bush unit length between the bush and the shaft. F_t is equal to kinetic force $F_t^k(V_w)$ if the relative velocity $|V_w| > 0$, whereas for $V_w = 0$ its values are located in the interval $[-F_t^s, F_t^s]$, where F_t^s denotes the maximal value of the static friction force:

$$F_t = \mathrm{Sgn}(V_w)\begin{cases} F_t^k(V_w) & \text{if } |V_w| > 0, \\ F_t^s & \text{if } |V_w| = 0, \end{cases} \quad \mathrm{Sgn}(V_w) = \begin{cases} 1 & \text{if } V_w > 0, \\ [-1, 1] & \text{if } V_w = 0, \\ -1 & \text{if } V_w < 0. \end{cases} \tag{3}$$

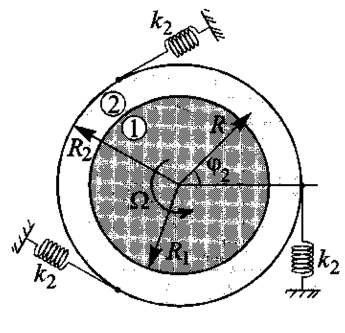

Fig. 1. A model of the problem.

We consider a one-dimensional model of thermal friction and wear during stick-slip motion taking into account the following assumptions:

1. The external excitation of the system allows for neglecting of the term $\rho\partial^2\mathbf{u}/\partial t^2$ in the Lamé equation (1). Shaft rotates with small angular velocity $\Omega(t)$ so that centrifugal forces $\rho\Omega^2 R$ could be neglected [23].
2. The vector components related to displacements as well as the shaft temperature do not depend on ϕ, Z, and the unequal zero components $U(R,t)$, $V(R,t)$ and $T(R,t)$ depend only on the radial co-ordinate and time.
3. We also assume that according to Coulomb's law friction force is proportional to normal part of reaction $F_t = f(V_w)N(t)$, with the following friction coefficient:

$$f(V_w) = \mathrm{Sgn}(V_w)\begin{cases} f_k(V_w) & \text{if } |V_w| > 0, \\ f_s & \text{if } V_w = 0, \end{cases} \tag{4}$$

   where f_s denotes maximal value of the static friction coefficient.
4. The coefficient of kinetic friction $f_k(V_w)$ is dependent on the relative velocity of shaft and bush in a way governed by equation $V_w = \Omega R_1 - \dot{\varphi}_2(t)R_1$ (see Fig. 2). The so-called Harsy–Stribeck's curve [3,5] has a minimum when $V_w = V_{\min}$, whereas for $V_w < V_{\min}$ friction coefficient decreases $f_k'(V_w) < 0$. Observe that rather various functions are taken in the literature to approximate the experimentally found values. It leads to different approximations of both friction force and momentum. The most popular is that governed by simple equation $f(V_w) = \mathrm{Sgn}(V_w)f_s$. A review of various friction models can be found in [3–6]. As a criterion choice of a friction model usually a minimal set of parameters together with a good agreement with the experiment are taken. The dependence of kinetic friction coefficient versus sliding velocity (Fig. 2) can be presented in the form

$$f_k(V_w) = \begin{cases} f_{\min} + (f_s - f_{\min})\exp(-b_1|V_w|) & \text{if } |V_w| \leqslant V_{\min}, \\ f_{\min} + (f_s - f_{\min})\exp(-b_1|V_{\min}|) + \frac{b_2 b_3(|V_w| - V_{\min})^2}{1 + b_2(|V_w| - V_{\min})} & \text{if } |V_w| > V_{\min}, \end{cases} \tag{5}$$

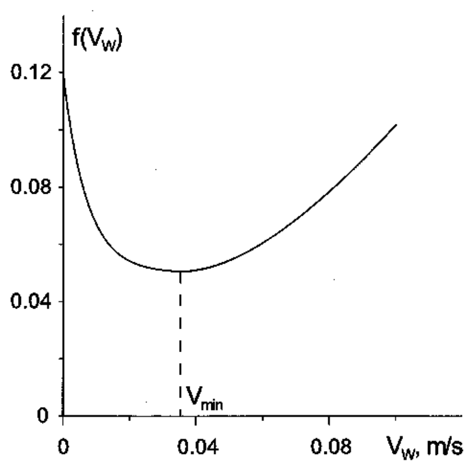

Fig. 2. Dependence of kinetic friction coefficient versus relative velocity.

where f_s, $f_{\min}$, b_1, b_2, b_3, $V_{\min}$ can be defined via experiment, and the function $f_k(V_w)$ is smooth for $|V_w| > 0$, $f_k(0+) = f_s$, $f_k(V_w)/V_w|_{V_w \to \infty} = b_3$.

For computation purposes, the multi-valued relation $\mathrm{Sgn}(x)$ is approximated by the function $\mathrm{Sgn}_{\varepsilon_0}(x)$ defined in [4]

$$\mathrm{Sgn}_{\varepsilon_0}(x) = \begin{cases} 1 & \text{if } x > \varepsilon_0, \\ \left(2 - \frac{|x|}{\varepsilon_0}\right)\frac{x}{\varepsilon_0} & \text{if } |x| < \varepsilon_0, \\ -1 & \text{if } x < -\varepsilon_0, \end{cases} \tag{6}$$

where $\varepsilon_0 = 0.0001$.

5. The heat flows q_1 and q_2 are generated on the contact surface due to Ling rule [24] and governed by the equation $q_1 + q_2 = (1 - \eta)F_{\mathrm{fr}}V_w$, where $\eta \in [0, 1]$ denotes the part of heat energy which goes on the wear [14]. Both flows q_1 and q_2 go into shaft and bush, respectively:

$$q_1 = \lambda_1 \frac{\partial T(R,t)}{\partial R}, \quad q_2 = -\alpha_T(T_0 - T(R_1,t)), \tag{7}$$

where λ_1 is the heat conduction, and α_T is the heat exchange coefficient between shaft and a bush.

6. One of the most popular wear models is governed by the equation

$$\dot{U}_z(t) = K_z|V_w(t)|^m P(t)^n, \tag{8}$$

where m, n are the exponents, K_z is the wear coefficient of the bush, and $P(t) = N(t)/2\pi R_1$ is the contact pressure. We assume Archard's law of wear [25,26] in the form of (8) where $m = n = 1$. The taken rule is typical for an abrasive wear.

After taking into account the above assumptions our problem (from a mathematical viewpoint) is governed by Eq. (1) which can be reduced to that of finding a solution to the quasi-static thermoelasticity equations [20] described in the cylinder co-ordinates of the form

$$\frac{\partial^2 U(R,t)}{\partial R^2} + \frac{1}{R}\frac{\partial U(R,t)}{\partial R} - \frac{1}{R^2}U(R,t) = \alpha_1 \frac{1+\nu}{1-\nu}\frac{\partial T(R,t)}{\partial R}, \tag{9}$$

$$\frac{\partial^2 T(R,t)}{\partial R^2} + \frac{1}{R}\frac{\partial T(R,t)}{\partial R} = \frac{1}{a_1}\frac{\partial T(R,t)}{\partial t}, \quad 0 < R < R_1, \ 0 < t < t_c. \tag{10}$$

The differential inclusion (2) is then approximated by the equation of bush movement as a solid body

$$B_2\ddot{\varphi}_2(t) + k_2R_2^2\varphi_2(t) = f(V_w)2\pi R_1^2 P(t), \quad 0 < t < t_c. \tag{11}$$

The following mechanical boundary conditions are attached to Eqs. (9)–(11):

$$U(0,t) = 0, \quad U(R_1,t) = -U_0h(t) + U_z(t), \qquad 0 < t < t_c \tag{12}$$

as well as both the heat boundary conditions

$$\lambda_1 \frac{\partial T(R_1,t)}{\partial R} + \alpha_T(T(R_1,t) - T_0) = (1-\eta)f(V_w)V_wP(t), \tag{13}$$

$$R\frac{\partial T(R,t)}{\partial R}\bigg|_{R\to 0} = 0, \quad 0 < t < t_c \tag{14}$$

and the initial conditions

$$T(R,0) = T_0,\ 0 < R < R_1, \quad \varphi_2(0) = \varphi_2^\circ, \quad \dot{\varphi}_2(0) = \omega_2^\circ. \tag{15}$$

A speed of bush or shaft wear is proportional to the power of friction force [25,26] in the following manner:

$$\dot{U}_z(t) = K_z|V_w(t)|P(t). \tag{16}$$

Radial stress $\sigma_R(R,t)$ in the cylinder can be determined after radial displacements $U(R,t)$ and temperature $T(R,t)$ in the cylinder as follows:

$$\sigma_R(R,t) = \frac{E_1}{1-2v}\left[\frac{1-v}{1+v}\frac{\partial U(R,t)}{\partial R} + \frac{v}{1-v}\frac{U(R,t)}{R} - \alpha_1(T(R,t) - T_0)\right]. \tag{17}$$

In the above expressions the following definitions are used: $P(t) = -\sigma_R(R_1,t)$, E_1 is the elasticity modulus, and v is Poisson's ratio. We find temperature, contact pressure, radial displacements, the velocity and the magnitude of wear at the moment of time $t \in [0,t_c]$, where t_c is time of contact $(0 < t < t_c,\ P(t) > 0)$.

Integrating (9) and taking into account (12) and (17) we can write down contact pressure as follows:

$$P(t) = \frac{2E_1\alpha_1}{1-2v_1}\frac{1}{R_1^2}\int_0^{R_1}[T(\xi,t) - T_0]\xi\,\mathrm{d}\xi + \frac{E_1}{(1-2v_1)(1+v_1)R_1}[U_0h(t) - U_z].$$

In the above expressions the following dimensionless values are introduced:

$$r = \frac{R}{R_1}, \quad \tau = \frac{t}{t_*}, \quad u = \frac{U}{U_0}, \quad u_z = \frac{U_z}{U_0}, \quad p = \frac{P}{P_*}, \quad \theta = \frac{T - T_0}{T_*}, \quad Bi = \frac{\alpha_T R_1}{\lambda_1},$$

$$k_z = \frac{\Omega_* P_* t_* K_z R_1}{U_0}, \quad \gamma = \frac{2(1-\eta)E_1\alpha_1 R_1^2 \Omega_*}{\lambda_1(1-2v)}, \quad \varepsilon = \frac{P_* t_* 2\pi R_1^2}{B_2\Omega_*}, \quad \tilde{\omega} = \frac{t_* a_1}{R_1^2}, \quad \varphi^\circ = \frac{\varphi_2^\circ}{\Omega_* t_*},$$

$$\omega^\circ = \frac{\omega_2^\circ}{\Omega_*}, \quad \varphi(\tau) = \frac{\varphi_2(t_*\tau)}{\Omega_* t_*}, \quad F(\omega_1 - \dot{\varphi}) = f(R_1\Omega_*(\omega_1 - \dot{\varphi})), \quad h(\tau) = h(t_*\tau),$$

where the corresponding characteristic parameters read:

$$t_* = \sqrt{\frac{B_2}{k_2R_2^2}}, \quad P_* = \frac{E_1U_0}{(1+v)(1-2v)R_1}, \quad T_* = \frac{U_0}{2\alpha_1(1+v)R_1}.$$

In the dimensionless form the considered problem has the form:

$$\ddot{\varphi}(\tau) + \varphi(\tau) = \varepsilon F(\omega_1 - \dot{\varphi})p(\tau, \dot{\varphi}), \quad 0 < \tau < \infty, \tag{18}$$

$$\varphi(0) = \varphi^\circ, \quad \dot{\varphi}(0) = \omega^\circ, \tag{19}$$

$$p(\tau, \dot{\varphi}) = h(\tau) - u_z(\tau) + \int_0^1 \theta(\xi, \tau)\xi \, d\xi, \quad 0 < \tau < \infty, \tag{20}$$

$$u_z(\tau) = k_z \int_0^\tau |\omega_1 - \dot{\varphi}(\tau)| p(\tau, \dot{\varphi}) \, d\tau, \quad 0 < \tau < \infty, \tag{21}$$

$$\frac{\partial^2 \theta(r,\tau)}{\partial r^2} + \frac{1}{r}\frac{\partial T\theta(r,\tau)}{\partial r} = \frac{1}{\tilde{\omega}}\frac{\partial \theta(r,\tau)}{\partial \tau}, \quad 0 < \tau < \infty, \ 0 < r < 1, \tag{22}$$

$$\frac{\partial \theta(1,\tau)}{\partial r} + Bi\theta(1,\tau) = \gamma F(\omega_1 - \dot{\varphi}(\tau))(\omega_1 - \dot{\varphi}(\tau))p(\tau, \dot{\varphi}), \quad 0 < \tau < \infty, \tag{23}$$

$$r\frac{\partial \theta(r,\tau)}{\partial r}\bigg|_{r\to 0} = 0, \ 0 < \tau < \infty, \quad \theta(r, 0) = 0, \ 0 < r < 1. \tag{24}$$

3. Solution of the problem

Applying the Laplace transform to nonlinear problem (20)–(24) (s – the transformation parameter)

$$\left\{\bar{\theta}(r,s), \bar{p}(s), \bar{u}_z(s), \bar{h}(s), \bar{q}(s)\right\} = \int_0^\tau \{\theta(r,\tau), p(\tau), u_z(\tau), h(\tau), q(\tau)\} e^{-s\tau} \, d\tau,$$

where nonlinear part has the form

$$q(\tau) = \gamma F(\omega_1 - \dot{\varphi})(\omega_1 - \dot{\varphi})p(\tau, \dot{\varphi}), \tag{25}$$

we obtain the solution in the form of Laplace transforms

$$\bar{\theta}(r,s) = G_\theta(r,s)\bar{q}(s), \quad \bar{p}(s) = \bar{h}(s) + G_u(s)\bar{q}(s),$$

$$G_\theta(r,s) = \frac{I_0(s_\omega r)}{\tilde{\omega}\Delta_1(s)}, \quad G_u(s) = \frac{\Delta_1(s)}{\tilde{\omega}\Delta_1(s)}, \tag{26}$$

$$\Delta_2(s) = \frac{I_1(s_\omega)}{s_\omega}, \quad \Delta_1(s) = s_\omega^2 \Delta_2(s) + BiI_0(s_\omega), \quad s_\omega = \sqrt{\frac{s}{\tilde{\omega}}},$$

where $I_0(x)$, $I_1(x)$ are the modified Bessel functions.

Performing the inverse Laplace transformation with the help of residua's and convolution theorems [27] one can find the following relations:

$$p(\tau,\dot{\varphi}) = h(\tau) - u_z(\tau) + \gamma\tilde{\omega}\int_0^\tau G_u(\tau-\xi)F(\omega_1-\dot{\varphi})p(\xi,\dot{\varphi})(\omega_1-\dot{\varphi})\,\mathrm{d}\xi, \tag{27}$$

$$\theta(r,\tau) = \gamma\tilde{\omega}\int_0^\tau G_\theta(r,\tau-\xi)F(\omega_1-\dot{\varphi})p(\xi,\dot{\varphi})(\omega_1-\dot{\varphi})\,\mathrm{d}\xi, \tag{28}$$

where

$$\{G_u(\tau), G_\theta(1,\tau)\} = \sum_{m=1}^{\infty}\frac{\{2Bi, 2\mu_m^2\}}{Bi+\mu_m^2}\mathrm{e}^{-\mu_m^2\tilde{\omega}\tau} \tag{29}$$

and μ_m are the characteristic equation roots $(m = 1,2,3,\ldots)$ of the equation

$$BiJ_0(\mu) - \mu J_1(\mu) = 0. \tag{30}$$

Thus, the stated problem is reduced to the solution of the system of nonlinear differential (18) and integral (27) equations taking into account Eq. (21) for the contact pressure $p(\tau)$ and the velocity $\dot{\varphi}(\tau)$. Temperature and wear could be found using expressions (28) and (21), respectively.

4. Steady-state solution analysis

4.1. Analysis of steady-state solution in case of wear absence ($k_z = 0$)

Consider the case $\omega_1(\tau) = \omega_1^\circ H(\tau)$, $h(\tau) = H(\tau)$; $H(\tau) = 1$, $\tau > 0$, $H(\tau) = 0$, $\tau < 0$. The steady-state solution is found for these input data when wear is absent (in Eqs. (18) and (22) terms consisting time derivatives are neglected)

$$p_{\mathrm{st}} = \frac{1}{1-v}, \quad \theta_{\mathrm{st}} = \frac{2v}{1-v}, \quad \varphi_{\mathrm{st}} = \frac{\varepsilon F(\omega_1^\circ)}{1-v},$$
$$\gamma_1 = \varepsilon F(\omega_1^\circ)/\omega_1^\circ, \quad v = \gamma\omega_1^\circ F(\omega_1^\circ)/2Bi. \tag{31}$$

For the determination of the solution's behavior the linearization of the problem was performed in the vicinity of steady-state point (31). Assume perturbations as follows: $h(\tau) = 1 + h^*(\tau)$,

$$\omega_1(\tau) = \omega_1^\circ + \omega_1^*(\tau), \quad |h^*| \ll 1, \quad |\omega_1^*| \ll 1.$$

Then a solution can be represented in the form

$$\varphi(r,\tau) = \varphi_{\mathrm{st}} + \varphi^*(\tau), \quad \theta(r,\tau) = \theta_{\mathrm{st}}(r) + \theta^*(r,\tau), \quad p(\tau) = p_{\mathrm{st}} + p^*(\tau), \tag{32}$$

where $|\varphi^*| \ll 1$, $|\theta^*| \ll 1$, $|p^*| \ll 1$. The right-hand sides of Eq. (18) and the boundary condition (23) were linearized. For perturbations we obtain the linear problem

$$\ddot{\varphi}^*(t) + \varphi^*(t) = \varepsilon F(\omega_1^\circ)p^*(\tau) + \varepsilon F'(\omega_1^\circ)p_{\mathrm{st}}(\omega_1^* - \dot{\varphi}^*), \quad 0 < \tau < \infty, \tag{33}$$

$$\varphi^*(0) = 0, \quad \dot{\varphi}^*(0) = 0, \tag{34}$$

$$p^*(\tau) = h^*(\tau) + \int_0^1 \theta^*(\xi, \tau)\xi \, d\xi, \quad 0 < \tau < \infty, \tag{35}$$

$$\frac{\partial^2 \theta^*(r,\tau)}{\partial r^2} + \frac{1}{r}\frac{\partial \theta^*(r,\tau)}{\partial r} = \frac{1}{\tilde{\omega}}\frac{\partial \theta^*(r,\tau)}{\partial \tau}, \quad 0 < \tau < \infty, \ 0 < r < 1, \tag{36}$$

$$\frac{\partial \theta^*(1,\tau)}{\partial r} + Bi\theta^*(1,\tau) = \gamma\Big[\omega_1^\circ F(\omega_1^\circ)p^* + p_{st}(\omega_1^* - \dot{\varphi}^*)(F(\omega_1^\circ) + \omega_1^\circ F'(\omega_1^\circ))\Big], \quad 0 < \tau < \infty, \tag{37}$$

$$r\frac{\partial \theta^*(r,\tau)}{\partial r}\bigg|_{r\to 0} = 0, \ 0 < \tau < \infty, \quad \theta^*(r,0) = 0, \ 0 < r < 1. \tag{38}$$

Applying Laplace transformation to the linear problem (33)–(38) (s – parameter of transformation) of the form

$$\left\{\bar{\theta}^*(r,s), \bar{p}^*(s), \bar{\varphi}^*(s), \bar{h}^*(s), \bar{\omega}_1^*(s)\right\} = \int_0^\tau \{\theta^*, p^*, \varphi^*, h^*, \omega_1^*\} e^{-s\tau} d\tau,$$

we obtain a solution in Laplace transforms

$$\bar{\varphi}^*(s) = G_{\varphi h}(s)\bar{h}^*(s) + G_{\varphi\omega}(s)\bar{\omega}_1^*(s), \tag{39}$$

$$\bar{p}^*(s) = G_{ph}(s)\bar{h}^*(s) + G_{p\omega}(s)\bar{\omega}_1^*(s), \tag{40}$$

$$\bar{\theta}^*(r,s) = G_{\theta h}(r,s)\bar{h}^*(s) + G_{\theta\omega}(s)\bar{\omega}_1^*(s), \tag{41}$$

where

$$\left\{G_{\varphi h}(s), G_{\varphi\omega}(s), G_{ph}(s), G_{p\omega}(s), G_{\theta h}(s), G_{\theta\omega}(s)\right\} = \frac{\{\cdot\}}{\Delta^*(s)},$$

$$\begin{aligned}\{\cdot\} = \Big\{&F(\omega_1^\circ)\Delta_1(s), p_{st}\big\lfloor \gamma F^2(\omega_1^\circ)\Delta_2(s) + F'(\omega_1^\circ)\Delta_1(s)\big\rfloor, \Omega_2(s)\Delta_1(s),\\ &\gamma\varepsilon(s^2+1)\Delta_2(s)\big(F(\omega_1^\circ) + \omega_1^\circ F'(\omega_1^\circ)\big)p_{st}, I_0(s_\omega)\gamma\omega_1^\circ F(\omega_1^\circ)\Omega_1(s),\\ &\gamma\varepsilon I_0(s_\omega)(s^2+1)p_{st}\big(F(\omega_1^\circ) + \omega_1^\circ F'(\omega_1^\circ)\big)\Big\}.\end{aligned} \tag{42}$$

The characteristic equation of the steady-state problem has the form

$$\begin{aligned}&\Delta^*(s) = 0, \quad \Delta^*(s) = \Delta_1(s)\Omega_2(s) - 2Biv\Delta_2(s)\Omega_1(s),\\ &\Omega_1(s) = s^2 - \frac{\gamma_1}{1-v}s + 1,\\ &\Omega_2(s) = s^2 + \frac{\gamma_2}{1-v}s + 1,\\ &\gamma_2 = \varepsilon F'(\omega_1^\circ).\end{aligned} \tag{43}$$

The roots s_m ($\mathrm{Re}s_1 > \mathrm{Re}s_2 > \cdots > \mathrm{Re}s_m > \cdots$, $m = 1,2,3,\ldots$) of the characteristic Eq. (43) can be located in the left-hand side $\mathrm{Re}s < 0$ (steady solution is stable) or the right-hand side $\mathrm{Re}s > 0$ (steady solution is unstable) of the complex plane depending on the input data of the problem. The parameters of the problem for which the roots transition takes place will be called further critical. The analysis of the parameter's regions of steady-state solution stability is carried out. The characteristic function is presented in the form

$$\Delta^*(s) = \sum_{m=0}^{\infty}\left(\frac{s}{\tilde{\omega}}\right)^m d_m,$$

$$d_m = (1-\delta_{m1})\tilde{\omega}^2\left(d_{m-2}^{(1)} - 2Biv d_{m-2}^{(2)}\right) + \frac{\tilde{\omega}}{1-v}\left(\gamma_2 d_{m-1}^{(1)} + 2Biv\gamma_1 d_{m-1}^{(2)}\right) + d_m^{(1)} - 2Biv d_m^{(2)}, \quad (44)$$

$$m = 1,2,\ldots,\quad \delta_{mn} = 1,\ m = n,\quad \delta_{mn} = 0,\ m \neq n,$$

$$d_0 = Bi(1-v),\quad d_m^{(1)} = \frac{Bi + 2m}{2^{2m}(m!)^2},\quad d_m^{(2)} = \frac{1}{2^{2m+1}m!(1+m)!}.$$

The dependence of critical value v versus parameter γ_2 for different $\tilde{\omega} = 0.05,\ 0.1,\ 1$ is presented in Fig. 3 (curves 1–3, correspondingly). Fig. 4 contains the dependence of critical value v versus parameter $\tilde{\omega}$ for different values $\gamma_2 = -0.05,\ -0.08$ (curves 1 and 2). The parameter $Bi = 10$, $\gamma_1 = 0.586$. For the parameters that are situated inside curves, a steady-state solution is stable. The detailed analysis shows that decreasing of γ_2 leads to narrowing the stability area according to parameter v and to increasing of critical values $\tilde{\omega}$. When $v = 0$ and neglecting heat expansion of the cylinder we obtain a model of self-oscillations [6], with the characteristic equation of the linearized problem $\Omega_2(s) = 0$. In this case a steady-state solution is stable, when $\gamma_2 > 0$. When $\tilde{\omega} = 0$ (bush is immovable) we obtain a model [12] with the characteristic equation $\Delta_1(s) - 2Biv\Delta_2(s) = 0$. In this case, when $v > 1$ a steady solution is unstable (root $s_1 > 0$). The so-

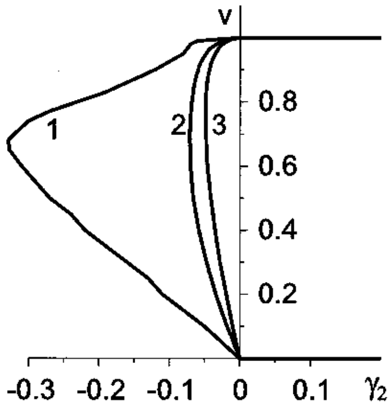

Fig. 3. Dependence of critical value of v versus critical value of γ_2 for different values of the parameter $\tilde{\omega}$ ($k_z = 0$). Curve 1: $\tilde{\omega} = 0.005$, 2: $\tilde{\omega} = 0.1$, 3: $\tilde{\omega} = 1$. The parameter regions inside the curves correspond to the area of steady-state solution stability.

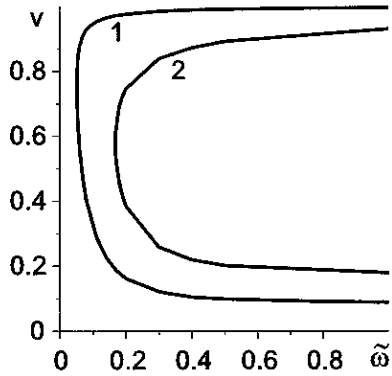

Fig. 4. Critical value of v dependence versus critical value of $\tilde{\omega}$ for different γ_2 ($k_z = 0$). Curve 1: $\gamma_2 = -0.05$, 2: $\gamma_2 = -0.08$. Regions of steady-state solution stability are inside the corresponding curves.

called thermal instability [12] or thermal explosion [14,15] takes place. The analysis of the particular cases of the considered model shows that from one side steady-state solution is stable, when $\gamma_2 > 0$. This corresponds to $V_w > V_{\min}$ (see Fig. 2). From the other side a steady solution is stable, when $v < 1$. The specific parameters of the system, the view of Stribeck's curve and analysis of the characteristic equation roots (43) can help definitely to answer the question about the stability of steady-state solution. If steady solution (31) is unstable, then after solving a transient problem it can behave as a stable limit cycle similar to frictional self-oscillations or it can increase with time.

4.2. Analysis of steady-state solution in the presence of wear ($k_z \neq 0$)

The steady-state solution of the problem in the case of presence of wear is found (in Eqs. (18) and (22) the terms with time derivatives and $\dot{u}_z(\tau) = 0$ are neglected)

$$p_{\rm st} = 0, \quad \theta_{\rm st} = 0, \quad \varphi_{\rm st} = 0, \quad u_z^{\rm st} = 1. \tag{45}$$

Performing similar to the previous case procedure the characteristic equation of linearized problem is obtained in the vicinity of steady solution (45)

$$\Delta^*(s) = 0, \quad \Delta^*(s) = (s + k_z\omega_1^\circ)\Delta_1(s) - 2Bivs\Delta_2(s). \tag{46}$$

The analysis of the parameter's regions in which steady-state solution (45) is stable is carried out. For this purpose the characteristic function is sought in the form

$$\Delta^*(s) = \sum_{m=0}^{\infty} \left(\frac{s}{\tilde{\omega}}\right)^m b_m, \tag{47}$$

$$b_0 = kd_0^{(1)}, \quad k = k_z\omega_1^\circ, \quad b_m = kd_m^{(1)} + \tilde{\omega}\left(d_{m-1}^{(1)} - 2Bivd_{m-1}^{(2)}\right), \; m = 1, 2, \ldots \tag{48}$$

First, a root of the characteristical equation for small wear $k \ll 1$ can be presented in the form

$$s_1 = -\frac{k}{1-v}. \tag{49}$$

As it can be seen from (49) for low wear when $v < 1$ the steady solution (45) is stable and in opposite case – unstable. In the conditions of wear presence system's contact time t_c is limited. The material of the bush will wear with time. That is why we should accurately state conditions of stability. Parameters of the problem under which roots s_1, s_2 of the characteristic equation have positive real part and they are complex conjugate are related to intensive wear. Under these parameters oscillation amplitude increases according to exponential law but system's contact time is limited. System will go out from the contact faster than contact characteristics will reach critical values (initial assumptions will lose sense). Parameters of the problem under which the roots of the characteristic equation s_1, s_2 have only positive real part are referred as the critical parameters. Under these parameters there will be no oscillations but contact characteristics will rise according to an exponential law. The system will be overheated. The rate of heat expansion is bigger than wear rate. In Fig. 5 the dependence of critical value v (solid curves) versus parameter k for different values of $\tilde{\omega} = 0.05,\ 0.1$ (curves 1 and 2, respectively) is presented. Taking into account three terms in the decomposition (47) the formula for critical values is derived (roots coincide on real axis $\mathrm{Re}\, s_1 = \mathrm{Re}\, s_2 > 0$, $\mathrm{Im}\, s_1 = \mathrm{Im}\, s_2 = 0$)

$$v_{\mathrm{cr}} = 1 + \frac{k + \sqrt{2Bik\tilde{\omega}(4+Bi)}}{2Bi\tilde{\omega}}.$$

This formula is the more accurate the less wear parameter k is. For the parameters that are situated under the solid curve $v < v_{\mathrm{cr}}$ the system is stable. Moreover, between solid and dashed curves $v_0 < v < v_{\mathrm{cr}}$ time, when the system is in contact is limited and intensive wear takes place.

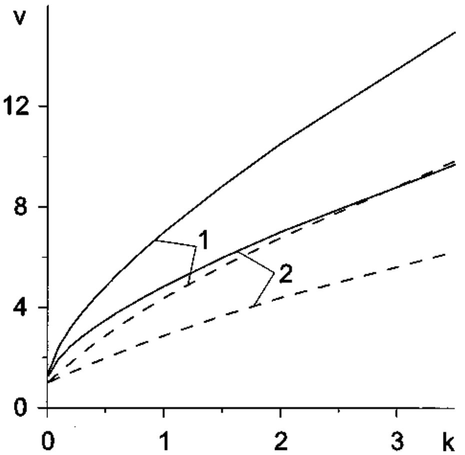

Fig. 5. Critical values v versus k for different $\tilde{\omega}$ ($k_z \neq 0$). Curves 1: $\tilde{\omega} = 0.05$, 2: $\tilde{\omega} = 0.1$. Regions under solid curves are stable. Parameter regions between solid and dashed curves correspond to intensive wear.

The formula for the dashed curve is also found (roots are transiting through imaginary axis $\mathrm{Re}\,s_1 = \mathrm{Re}\,s_2 = 0$, $\mathrm{Im}\,s_1 = -\mathrm{Im}\,s_2 \neq 0$)

$$v_0 = 1 + \frac{k(2+Bi)}{4Bi}.$$

This formula is the more accurate the less wear parameter k is.

5. Numerical analysis of the transient solution

The numerical analysis of the problem is performed using Runge–Kutta method by taking into account the following asymptotes:

$$G_\theta(1,\tau) \approx \sqrt{1/\pi\tau\tilde{\omega}}, \qquad G_u(\tau) \approx 1, \quad \tau \to 0.$$

The following kinetic friction parameters have been fixed: $f_s = 0.12, f_{\min} = 0.05$, $b_1 = 140$ s m^{-1}, $b_2 = 10$ s m^{-1}, $b_3 = 2$ s m^{-1}, $V_{\min} = 0.035$ m c^{-1}.

The results of calculations for different values of the parameter $\gamma = 0$, 200, 400 for the steel cylinder ($\alpha_1 = 14 \times 10^{-6}$ °C^{-1}, $\lambda_1 = 21$ W/(m °C^{-1}), $\nu = 0.3$, $a_1 = 5.9 \times 10^{-6}$ m^2/s, $E_1 = 19 \times 10^{10}$ Pa) and $R_1 = 0.03$ m, $\Omega = 1$ rad/s, $\varepsilon = 10$, $\tilde{\omega} = 0.1$, $Bi = 10$, $\varphi^\circ = 0$, $\omega^\circ = 0$ are shown in Figs. 6–14. Solid curves correspond to the case of wear absence $k_z = 0$, dashed – to the case of wear with the dimensionless wear coefficient $k_z = 0.1$. In this case $t_* = 0.25$ s, $P_* = 1.22 \times 10^4$ Pa, $\gamma_1 = 0.51$, $\gamma_2 = -196$.

In the case of heat expansion absence time evolutions of the dimensionless speed $\dot{\varphi}(\tau)$ (curve 1), dimensionless displacement $\varphi(\tau)$ (curve 2) of the bush and dimensionless friction force $\varepsilon F(\omega_1 - \dot{\varphi})p(\tau)$ (dashed curve 3) for $\gamma = 0$ ($v = 0$, $s_1 = 0.0051$ the steady-state solution is unstable) are shown in Fig. 6.

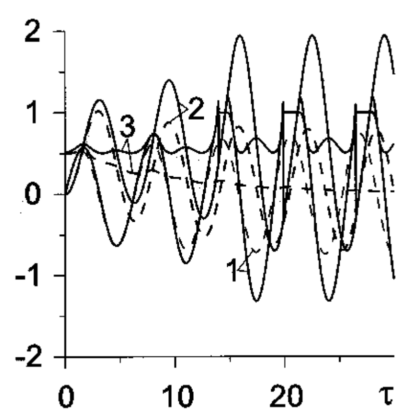

Fig. 6. Dependence of bush movement dimensionless velocity $\dot{\varphi}$ (curve 1), dimensionless displacements φ (curves 2) and dynamic friction force $\varepsilon F(\omega_1 - \dot{\varphi})$ (curve 3) versus dimensionless time τ in conditions of heat expansion absence $\gamma = 0$. Solid curves: $k_z = 0$, dashed curves: $k_z = 0.1$.

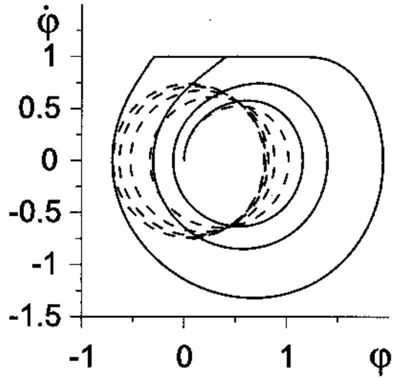

Fig. 7. Phase trajectory of bush movement in conditions of heat expansion absence $\gamma = 0$. Solid curves: $k_z = 0$, dashed curves: $k_z = 0.1$.

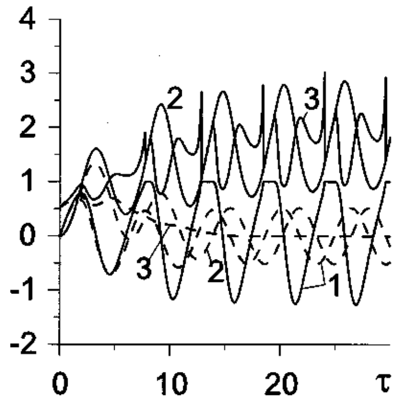

Fig. 8. Dependence of bush dimensionless velocity $\dot{\varphi}$ (curves 1), dimensionless displacements φ (curve 2) and dynamic friction force $\varepsilon F(\omega_1 - \dot{\varphi})$ (curve 3) versus dimensionless time τ, when $\gamma = 200$. Solid curves: $k_z = 0$, dashed curves: $k_z = 0.1$.

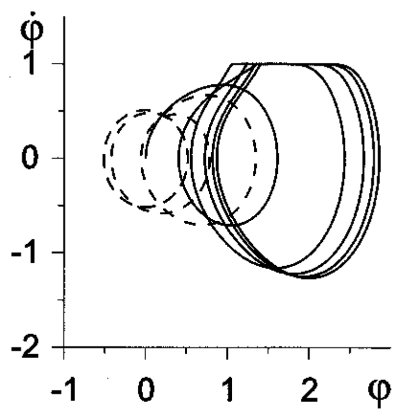

Fig. 9. Phase trajectory of bush movement in conditions, when $\gamma = 200$. Solid curves: $k_z = 0$, dashed curves: $k_z = 0.1$.

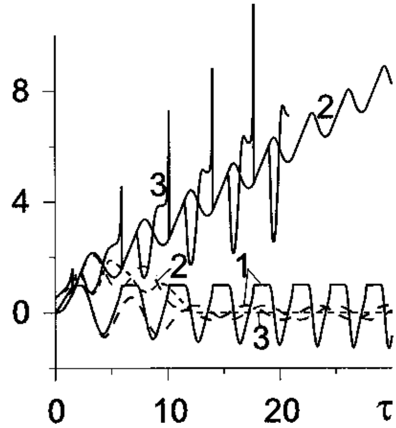

Fig. 10. Dependence of bush dimensionless velocity $\dot{\varphi}$ (curve 1), dimensionless displacements φ (curve 2) and dynamic friction force $\varepsilon F(\omega_1 - \dot{\varphi})$ (curve 3) versus dimensionless time τ when $\gamma = 400$. Solid curves: $k_z = 0$, dashed curves: $k_z = 0.1$.

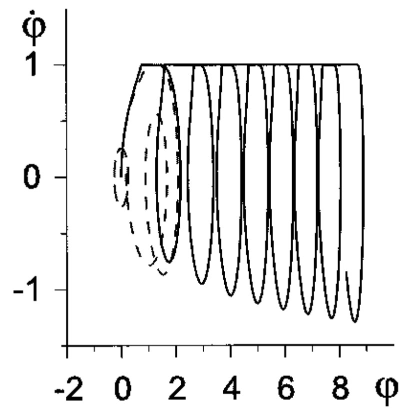

Fig. 11. Phase trajectory of bush movement for $\gamma = 400$. Solid curves: $k_z = 0$, dashed curves: $k_z = 0.1$.

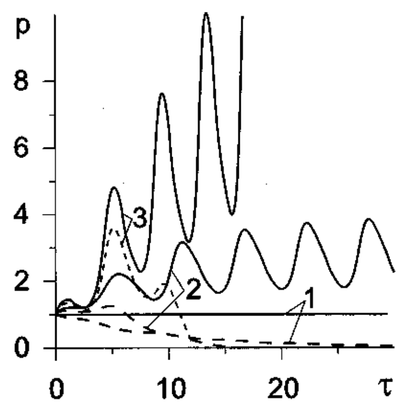

Fig. 12. Behavior of dimensionless contact pressure p versus dimensionless time τ for different values of γ. Curve 1: $\gamma = 0$, 2: $\gamma = 200$, 3: $\gamma = 400$. Solid curves: $k_z = 0$, dashed curves: $k_z = 0.1$.

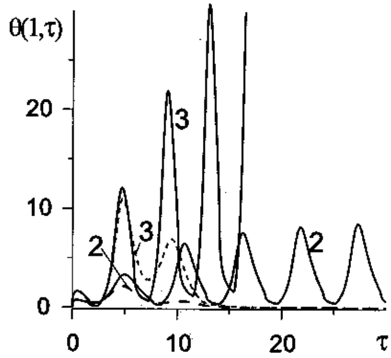

Fig. 13. Behavior of dimensionless contact temperature $\theta(1,\tau)$ versus dimensionless time τ for different values of parameter γ. Curve 2: $\gamma = 200$, 3: $\gamma = 400$. Solid curve: $k_z = 0$, dashed curves: $k_z = 0.1$.

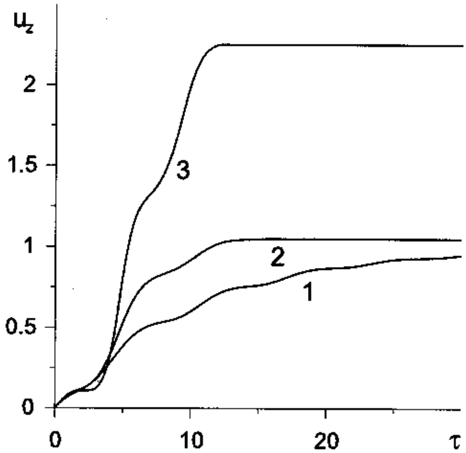

Fig. 14. Time evolution of dimensionless wear u_z for different values of parameter γ. Curve 1: $\gamma = 0$, 2: $\gamma = 200$, 3: $\gamma = 400$.

Fig. 7 illustrates the behavior of the phase trajectory in the phase plane without taking into account heat expansion of the cylinder $\gamma = 0$ and wear of the bush $k_z = 0$ (solid curve) and with wear (dashed curve). In conditions of wear absence a transient solution leads with time to stable limit cycle with the period 6.608. Stick-slip phenomenon takes place. Let us point out that (as it can be seen from this figure) the friction force has a jump at the instant of time when bush speed reaches speed of the cylinder $V_w = 0$. At that moment the rest friction force changes the sign. Then dimensionless friction force becomes equal to dimensionless displacement and this lasts to the moment when it reaches maximal value of static friction force. From that instant of time friction force decreases. After that it reaches local minimum when bush acceleration is equal to zero. Then friction force increases until it reaches cylinder's velocity $V_w = 0$. Process continues cyclically. In conditions of wear presence friction force will tend with time to zero and bush will perform its own oscillations with the period of 2π. Time evolutions of the dimensionless speed $\dot{\varphi}(\tau)$ (curve 1), dimensionless displacement $\varphi(\tau)$ (curve 2) of the bush and dimensionless dynamic friction force $\varepsilon F(\omega_1 - \dot{\varphi})p(\tau)$ (dashed curve 3) are shown in Fig. 8 for $\gamma = 200$ ($v = 0.51$, $s_1 = 0.0012$ steady-state solution is unstable). Fig. 9 illustrates the behavior of the phase trajectory in phase plane without taking into account a heat expansion of the cylinder $\gamma = 200$ and $k_z = 0$ (solid curve) and with wear (dashed line). As it can be seen in conditions of bush wear absence the contact characteristics tend with time to the limit cycle with the period equal to 5.5.

Fig. 10 illustrates changing with time of the dimensionless speed $\dot{\varphi}(\tau)$ (curve 1), dimensionless displacement $\varphi(\tau)$ (curve 2) of the bush and dimensionless dynamic friction force $\varepsilon F(\omega_1 - \dot{\varphi})p(\tau)$ (dashed curve 3) for $\gamma = 400$ ($v = 1.02$, $s_1 = 2 \times 10^{-6}$). Fig. 11 illustrates the behavior of phase trajectory on phase plane without taking into account the heat expansion of the cylinder $\gamma = 400$ and $k_z = 0$ (solid curve) and with wear (dashed curve). In the case of wear absence thermoelastic instability takes place. System's characteristics do not tend with time to stable limit cycle but exponentially increase. In that case cylinder does not have enough time to become cool. Wear presence (dashed curves) leads to thermoelastic instability disappearing.

Time changing laws for the contact pressure, temperature and wear are shown in Figs. 12–14 by solid (dashed) curves for the case of wear absence (presence), correspondingly. Curve 1 corresponds to the case of absence of heat expansion $\gamma = 0$, curve 2 to $\gamma = 200$, curve 3 to $\gamma = 400$. In the last case contact characteristics increase and cylinder does not have time for cooling. While parameter $\tilde{\omega}$ decreases and $v < 1$ time necessary for leading of contact characteristics on limit cycle increases. Wear presence leads to decreasing of contact characteristic values and to limiting of system's contact time (curves 2 and 3 in Fig. 12). With the increasing of the parameter γ system's contact time decreases and, correspondingly, bush wear increases and its value becomes bigger than value of initial deformation caused by an initial stress state of the cylinder.

6. Conclusions

New model of thermoelastic contact, in which changes of bush movement velocity, contact pressure, friction force, contact temperature and wear are mutually connected, is considered. Frictional self-oscillations arising conditions are investigated. In wear absence these conditions (at the same time they are conditions of steady-state solution stability) are also conditions of linearized problem characteristic equation roots transition from left-hand side ($\mathrm{Re}\, s_1 < 0$) to right-hand side ($\mathrm{Re}\, s_1 > 0$) of Laplace transformation parameter complex plane. In conditions of wear presence stick-slip movements disappear with time. System's contact time is limited. The upper bound of the solution stability conditions can be conditions of coinciding of first roots of characteristical equation $\mathrm{Im}\, s_1 = \mathrm{Im}\, s_2 = 0$, $\mathrm{Re}\, s_1 = \mathrm{Re}\, s_2 > 0$ in the right-hand side of the complex plane. Taking into account a heat expansion of the cylinder and wear of bush extends regions for the parameters in which steady-state solution is stable, i.e., heat expansion and wear play role of stabilizing factors.

References

[1] J. Awrejcewicz, I.V. Andrianov, L.I. Manievich, Asymptotic Approaches in Nonlinear Dynamics: New Trends and Applications, Springer, Berlin, 1998.

[2] J. Awrejcewicz, Deterministic Oscillations of the Discrete Systems, Warsaw, 1996 (in Polish).

[3] I. Krahelskyy, N. Hittis, Frictional Self-Oscillations, Moscow, 1987 (in Russian).
[4] J.A.C. Martins, J.T. Oden, F.M.F. Simões, Int. J. Eng. Sci. 28 (1990) 29.
[5] R.A. Ibrahim, Appl. Mech. Rev. 47 (1994) 209.
[6] A. Andronov, A. Vitt, C. Chaikin, Theory of Oscillations, Moscow, 1981 (in Russian).
[7] A.V. Chichinadze, E.D. Brown, A.H. Hinsburg, Z.V. Ihnatyeva, Calculation, Trial and Selection of Friction Couples, Nauka, Moskow, 1979.
[8] J. Awrejcewicz, Sci. Bull. Łódź Technical University 66 (1983) 21 (in Polish).
[9] J. Awrejcewicz, Sci. Bull. Łódź Technical University 72 (1987) 5.
[10] J. Awrejcewicz, KSME J. 2 (1988) 104.
[11] J. Awrejcewicz, J. Delfs, Eur. J. Mech. A/Solids 9 (1990) 269.
[12] Yu. Pyryev, D. Hrylitskyy, Appl. Mech. Techn. Phys. 37 (1996) 99 (in Russian).
[13] Yu. Pyryev, Physico-Chem. Mech. Mater. 36 (2000) 53 (in Russian).
[14] V. Alexandrov, H. Annakulova, Friction Wear 11 (1990) 24 (in Russian).
[15] V. Alexandrov, H. Annakulova, Friction Wear 13 (1992) 154 (in Russian).
[16] Yu. Pyryev, Friction Wear 15 (1994) 941 (in Russian).
[17] Z.S. Olesiak, Yu.A. Pyryev, in: Proceedings of the Third International Congress of Thermal Stresses, Cracow, Poland, June 13–17, 1999, p. 599.
[18] Z.S. Olesiak, Yu.A. Pyryev, Acta Mech. 143 (2000) 67.
[19] Z. Olesiak, Yu. Pyryev, A. Yevtushenko, Wear 210 (1997) 120.
[20] A. Kovalenko, Thermoelasticity, Kyyiv, 1975 (in Russian).
[21] A.F. Ulitko, Mech. Solid Body 6 (1990) 55 (in Russian).
[22] M. Kunze, Non-smooth Dynamical Systems, Springer, Berlin, 2000.
[23] S. Timoshenko, J.N. Goodier, Theory of Elasticity, McGraw-Hill, New York, 1951.
[24] F.F. Ling, ZAMP 10 (1959) 461.
[25] J.F. Archard, ZAMP 2 (1959) 438.
[26] I.H. Horyacheva, M. Dobychin, Contact Problems in Tribology, Mashynostroyeniye, Moskow, 1988 (in Russian).
[27] H.S. Carslaw, J.C. Jaeger, Conduction of Heat in Solids, Clarendon Press, Oxford, 1959.